Published in final edited form as:
Biochem Pharmacol. 2013 April 15; 85(8): 1195–1202. doi:10.1016/j.bcp.2013.01.031.

Comparative in vitro metabolism of phospho-tyrosol-indomethacin by mice, rats and humans

Gang Xie[1], **Dingying Zhou**[1], **Ka-Wing Cheng**[1], **Chi C. Wong**, and **Basil Rigas**[1,2,3]

[1]Division of Cancer Prevention, Department of Medicine, Stony Brook University, Stony Brook, NY 11794, USA

[2]Medicon Pharmaceuticals, Inc., Stony Brook, NY 11790, USA

Abstract

Phospho-tyrosol-indomethacin (PTI; MPI 621), a novel anti-cancer agent, is more potent and safer than conventional indomethacin. Here, we show that PTI was extensively metabolized *in vitro* and *in vivo*. PTI was rapidly hydrolyzed by carboxylesterases to generate indomethacin as its major metabolite in the liver microsomes and rats. PTI additionally undergoes cytochromes P450 (CYP)-mediated hydroxylation at its tyrosol moiety and *O*-demethylation at its indomethacin moiety. Of the five major human CYPs, CYP3A4 and CYP2D6 catalyze the hydroxylation and *O*-demethylation reactions of PTI, respectively; whereas CYP1A2, 2C9 and 2C19 are inactive towards PTI. In contrast to PTI, indomethacin is primarily *O*-demethylated by CYP2C9, which prefers acidic substrates. The hydrolyzed and *O*-demethylated metabolites of PTI are further glucuronidated and sulfated, facilitating drug elimination and detoxification. We observed substantial inter-species differences in the metabolic rates of PTI. Among the liver microsomes from various species, PTI was the most rapidly hydrolyzed, hydroxylated and *O*-demethylated in mouse, human and rat liver microsomes, respectively. These results reflect the differential expression patterns of carboxylesterase and CYP isoforms among these species. Of the human microsomes from various tissues, PTI underwent more rapid carboxylesterase-and CYP-catalyzed reactions in liver and intestine microsomes than in kidney and lung microsomes. Together, our results establish the metabolic pathways of PTI, reveal significant inter-species differences in its metabolism, and provide insights into the underlying biochemical mechanisms.

Keywords

phospho-tyrosol-indomethacin; cytochrome P450; liver microsomes; glucuronidation

1. Introduction

Inflammatory responses play critical roles in tumorigenesis, and nonsteroidal anti-inflammatory drugs (NSAIDs) inhibit cancer progression and its malignant conversion [1].

[3]Corresponding author, Basil Rigas, Stony Brook University, Division of Cancer Prevention, HSC, T17-080; Stony Brook, NY 11794-8173, USA, Tel: 1-631-444-9538; Fax: 1-631-444-9553; basil.rigas@stonybrook.edu.

Statement of conflicts of interest: The authors have nothing to disclose except for BR, who has an equity position in Medicon, Pharmaceuticals, Inc.

In 1976, indomethacin (IND), a well-known NSAID, was reported to inhibit growth of experimental tumors in mouse [2]. Following that, IND has been reported to be effective against various cancers, including those of colon [3], breast [4], lung [5] and skin [6]. IND inhibits tumor development at different stages including tumor initiation and promotion [7], invasion [8] and metastasis [9]. Mechanistically, it inhibits cancer cell proliferation and induces cancer cell apoptosis [10].

Despite the promising anti-cancer properties of IND, it has significant dose-limiting toxicity, particularly gastrointestinal toxicity due to its strong ability to inhibit cyclooxygenase-catalyzed synthesis of prostaglandins. In order to reduce its toxicity and improve its anticancer efficacy, we chemically modified IND at its –COOH group. Phospho-tysosol-IND (PTI) consists of IND with a diethylphosphate group covalently linked to it via a tyrosol spacer (Fig. 1A inset). Our preclinical study has demonstrated that PTI strongly inhibits colon and lung cancer in mice, and showed markedly reduced gastrointestinal toxicity compared to conventional IND [11].

Given the important role of drug metabolism in defining drug efficacy and toxicity, we systematically examined the metabolism of PTI *in vitro* using mouse, rat and human microsomes from various tissues, as well as *in vivo* in rats. Our findings reveal extensive biotransformations of PTI and significant inter-species differences in its metabolism, and provide insights into the biochemical mechanisms underlying its metabolic transformations.

2. Materials and Methods

2.1. Reagents

PTI was synthesized as reported [11]. IND, demethyl-IND, debenzoyl-IND, demethyldebenzoyl-IND, IND glucuronide, diisopropyl fluorophosphates (DFP), ketoconazole and quinidine were purchased from Toronto Research Chemicals (Toronto, Canada). 3'-phosphoadenosine-5'-phosphosulfate lithium salt, trifluoroacetic acid, and CH_3CN of HPLC grade were purchased from Sigma-Aldrich, St. Louis, MO. Mouse, rat and human liver microsomes, human liver cytosol, recombinant human CYPs (CYP1A2, 2C9, 2C19, 2D6 and 3A4), UGT2B7, NADPH regenerating solution, and UGT reaction solution were purchased from BD Biosciences, San Jose, CA. Human intestine, kidney and lung microsomes were purchased from XenoTech LLC (Lenexa, KS).

2.2. HPLC-UV analysis

The HPLC system consisted of a Waters Alliance 2695 Separations Module equipped with a Waters 2998 photodiode array detector (260 nm) and a Thermo Hypersil BDS C18 column (150 × 4.6 mm, particle size 3 μm). The mobile phase consisted of a gradient between aqueous phase (Trifluoroacetic acid, CH_3CN, H_2O (0.1:4.9:95 v/v/v)) and CH_3CN at a flow rate of 1 ml/min at 30°C. We applied gradient elution from 0% to 100% CH_3CN for 15 min, and it was maintained at 100% CH_3CN for 5 min.

2.3. LC-MS/MS analysis

The LC-MS/MS system consisted of Thermo TSQ Quantum Access (Thermo-Fisher) triple quadrupole mass spectrometer interfaced by an electrospray ionization probe with an Ultimate 3000 HPLC system (Dionex Corporation, Sunnyvale, CA). Chromatographic separations were achieved using a Luna C18 column (150 × 2 mm), and the mobile phase consisted of a gradient from 10% to 95% CH_3CN.

2.4. The metabolism of PTI by mouse, rat and human liver microsomes and human intestine, kidney and lung microsomes

PTI was preincubated at 37°C for 5 min with NADPH-regenerating solution (1.3 mM NADP, 3.3 mM D-glucose 6-phosphate, 3.3 mM $MgCl_2$, and 0.4 U/ml glucose-6-phosphate dehydrogenase) in 0.1 M potassium phosphate buffer (pH 7.4). The reaction was initiated by the addition of mouse, rat and human liver microsomes (protein concentration 0.5 mg/ml) or human intestine, kidney, and lung microsomes (protein concentration 0.25 mg/ml) and samples were maintained at 37°C for various time periods. At each of the designated time-points, 0.1-ml aliquots were mixed with 0.2 ml of CH_3CN, vortexed, and then centrifuged for 10 min at 13,000 × g. The supernatants were subjected to HPLC analyses. The HPLC peaks corresponding to each metabolite of PTI were collected and subjected to mass spectrometry analysis.

2.5. Stability of PTI in liver and intestinal microsomes

The half-life ($t_{1/2}$) of PTI was determined by non-linear regression analysis using one-phase decay model (GraphPad Prism, version 5). Intrinsic clearance (CL_{int}) of PTI was calculated using the formula $CL_{int} = (0.693/t_{1/2}) \times (V/P)$, where V is the incubation volume, and P is the mass of microsomal proteins in the incubation mixture.

2.6. Enzymatic kinetics of the metabolism of PTI by human CYP isoforms

Human recombinant CYPs were pre-incubated with diisopropyl fluorophosphates (DFP) (final 200 μM) at 37°C for 15 min to abrogate their esterase activities, and were subsequently treated with PTI ranging from 2 to 200 μM and an NADPH-regenerating solution in 0.1 M potassium phosphate buffer (pH 7.4) for 1 h. The resultant reaction mixtures (100 μl) were mixed with 200 μl CH_3CN, vortexed, and then centrifuged for 10 min at 13,000 × g. The supernatants were subjected to HPLC analysis. The kinetic parameters K_m and V_{max} were calculated using a nonlinear curve fitting program based on the Michaelis-Menten equation (GraphPad Prism 5.0; GraphPad Software Inc., San Diego, CA).

2.6. Glucuronidation of PTI by human liver microsomes

PTI was preincubated at 37°C for 5 min with UGT reaction solution (UDP glucuronic acid 2 mM, alamethicin 25 μg/ml and $MgCl_2$ 8mM) in 50 mM Tris-HCl buffer (pH 7.5). The reaction was initiated by the addition of human liver microsomes (protein concentration 0.5 mg/ml) and samples were maintained at 37°C for various time periods. At the end of each of the incubations, 0.1-ml aliquots were mixed with 0.2 ml of CH_3CN, vortexed, and then centrifuged for 10 min at 13,000 × g. The supernatants were subjected to HPLC analyses.

2.7. Preparation of demethyl-IND sulfate

Demethyl-IND (100 μM) was incubated with human liver cytosol (1 mg protein/ml) and 3'-phosphoadenosine-5'-phosphosulfate lithium salt (100 μM) in 100 mM Tris-HCl buffer (pH 7.4) at 37°C for 7 h. The resulting reaction mixture was deproteinized by adding acetonitrile prior to HPLC fractionation. The structure of the HPLC peak corresponding to demethyl-IND sulfate was confirmed by LC-MS/MS analysis.

2.8. The metabolism of PTI in rats

All animal care and experimental procedures were approved by the Institutional Animal Care and Use Committee at Stony Brook University. An equimolar single dose of PTI (10 mg/kg) or conventional IND (5 mg/kg) in corn oil was administered orally to rats, which were then sacrificed 3 h post-dosing. Rat blood was collected and immediately centrifuged.

The resulting plasma was deproteinized by immediate mixing it with a 2-fold volume of CH_3CN, and then subjected to HPLC analyses.

2.9. Statistical analysis

Results were analyzed using the Student's t-test; $p \leq 0.05$ was considered statistically significant.

3. Results

3.1. Phase I metabolism of PTI by mouse, rat and human liver microsomes

We first explored the metabolism of PTI by mouse, rat and human liver microsomes. PTI was rapidly hydrolyzed at its carboxylester bond to yield IND by the liver microsomes (Fig. 1A). Twenty minutes after initiation of the reactions, 22%, 52%, and 80% of PTI was hydrolyzed to yield IND by rat, human and mouse liver microsomes, respectively. Esterase-mediated hydrolysis of PTI essentially accounted for its microsomal instability. Consequently, the half-life ($t_{1/2}$) of PTI in liver microsomes decreased in the order: rat>human>mouse (Table 1).

In addition to IND, multiple minor metabolites of PTI were identified by LC-MS/MS analysis, including demethyl-PTI, debenzoyl-PTI and hydroxy-PTI (Fig. 2). Thus, PTI undergoes hydrolysis at its carboxylester bond, hydroxylation at its tyrosol moiety, O-demethylation and N-debenzoylation reactions at its IND moiety in liver microsomes, with its hydrolysis being the major reaction. Demethyl-PTI and hydroxy-PTI shared similar kinetic features in liver microsomes (Fig. 1B). Their levels increased rapidly reaching their peak values ~20 min after initiation of reaction, then decreased dramatically due to esterase-mediated hydrolysis. Of the microsomes from the three species, human liver microsomes (HLMs) generated by far the highest hydroxy-PTI level, while rat liver microsomes generated the highest demethyl-PTI level.

To determine whether these metabolic reactions are NADPH-dependent, we also examined the metabolism of PTI by HLMs in the absence of NADPH. Hydroxy-PTI, demethyl-PTI and demethyl-IND were not detected in the absence of NADPH, whereas debenzoyl-IND was detected (Fig. 1C). Thus, the hydroxylation and *O*-demethylation reactions of PTI and IND are NADPH-dependent, while the *N*-debenzoylation reaction is not.

3.2. Phase I metabolism of PTI by human intestine, kidney and lung microsomes

PTI was efficacious against human colon and lung cancer in preclinical models [11]. Therefore, we examined the metabolism of PTI in human intestine, lung and kidney microsomes. The dominant metabolic reaction of PTI in these microsomes is its hydrolysis to yield IND; the hydrolysis rate decreased in the order: intestine>kidney>lung (Fig. 3). As a result, intrinsic clearance (CL_{int}) of PTI in human intestine microsomes is much higher than that in human kidney and lung microsomes (Table 1). Minimal levels of demethyl-PTI and hydroxy-PTI were also detected in PTI-treated human intestine microsomes, but not in human kidney and lung microsomes (Fig. 3).

3.3. The metabolism of PTI by human CYPs

Cytochrome P450s (CYPs) are major drug-metabolizing enzymes that account for ~75% of the metabolism of clinically used drugs and other xenobiotics [12]. We evaluated the metabolism of PTI by five major human CYPs. The recombinant CYPs contained significant esterase activity, resulting in substantial hydrolysis of PTI. Therefore, we pre-treated CYPs with diisopropyl fluorophosphate (DFP) to inhibit the esterase activity, and then examined the kinetics of PTI metabolite formation by CYPs. As shown in Table 2, CYP3A4

exclusively catalyzed the hydroxylation PTI, while CYP2D6 predominantly catalyzed its *O*-demethylation. In contrast, CYP1A2, 2C9 and 2C19 were not appreciably active towards PTI.

We next evaluated the effects of ketoconazole (CYP3A4 inhibitor) and quinidine (CYP2D6 inhibitor) on the metabolism of PTI by HLMs. We observed that ketoconazole (10 μM) inhibited CYP3A4 activity by 98.0 %, and that quinidine (20 μM) inhibited CYP2D6 activity by 98.5%. We then evaluated the effects of these inhibitors on PTI metabolism by DFP-treated HLMs. Ketoconazole (10 μM) inhibited the hydroxylation of PTI in HLMs by 97.4%. Quinidine (20 μM) inhibited the *O*-demethylation of PTI in HLMs by 61.5%. These results indicate that CYP3A4 and CYP2D6 play major roles in the hydroxylation and O-demethylation of PTI by HLMs, respectively.

3.4. Glucuronidation reaction in human liver and intestinal microsomes

As NSAIDs can be glucuronidated at their free –COOH group, we examined the metabolism of PTI in the presence of UDP-glucuronic acid in HLMs. PTI was rapidly hydrolyzed to yield IND, which was then significantly glucuronidated (Fig. 4A). The level of IND glucuronide increased steadily throughout the entire period of observation. Human intestine microsomes generated similar results (data not shown). However, PTI itself is not glucuronidated, as evidenced by a lack of glucuronidation in the presence of DFP (Fig. 4B). Likewise, UDP-glucuronosyltransferase (UGT 2B7) was capable of catalyzing the glucuronidation of IND, but not that of PTI. Thus, the free –COOH group of IND is required for its acyl glucuronidation.

3.5. The metabolism of PTI in rats

An equimolar single dose of PTI or IND was administered orally to rats, which were sacrificed 3 h post-dosing. In rat plasma, we detected six metabolites: IND, demethyl-IND, debenzoyl-IND, demethyl-IND glucuronide, demethyl-IND sulfate and IND glucuronide (Fig. 5). Demethyl-IND glucuronide and demethyl-IND sulfate were identified by LC-MS/MS analysis (Fig. 6). We also prepared authentic demethyl-IND glucuronide and demethyl-IND sulfate by treating demethyl-IND with liver microsomes and cytosol, respectively, and their structures were confirmed using LC-MS/MS analysis. The plasma level of IND was significantly higher than that of any other metabolites ($P<0.01$) following IND or PTI administration (Fig. 5). PTI and IND generated similar metabolite level in rat plasma. Intact PTI, however, was not detected in the rat plasma.

4. Discussion

This work establishes the metabolic pathways of PTI *in vitro* and *in vivo*. As illustrated in Fig. 7, PTI undergoes the following metabolic reactions: 1) *hydrolysis* at its carboxylester bond to yield IND; 2) *O-demethylation* to form demethyl-PTI; 3) *hydroxylation* at its tyrosol moiety to form hydroxy-PTI; 4) *N-debenzoylation* to form debenzoyl-PTI; and 5) *phase II glucuronidation and sulfation* of IND and demethyl-IND to form conjugated metabolites.

The rapid hydrolysis of PTI to IND is catalyzed by carboxylesterase (CES) [13]. In mammals, there are two major isoforms of CES, CES1 (liver) and CES2 (intestine). CES1 mainly catalyzes the hydrolysis of esters with a large acyl group, while CES2 prefers substrates with bulky alcohol group. Liver is a major site for CES-mediated drug elimination. While the expression of CES1 in liver is similar in mouse, rat and human, the liver expression of CES2 decreases in the order: mouse>human>rat [14]. As both CES1 and CES2 can efficiently hydrolyze PTI [13], it is reasonable to observe that the hydrolysis rates of PTI in liver microsomes from various species decreased in the order: mouse>human>rat.

The human intestine microsomes are also highly efficient in hydrolyzing PTI, likely a result of high expression of CES2 in human intestine [15]. In comparison, the expressions of CES1 and CES2 are considerably lower in human kidney and lung [15], thus accounting for the higher stability of PTI in these microsomes.

CYPs also play a major role in the phase I metabolism of PTI by catalyzing its hydroxylation and *O*-demethylation. Of the five major human CYPs, CYP3A4 uniquely catalyzes the hydroxylation of PTI at its tyrosol moiety, presumably because the active site of CYP3A4 is large and flexible. Indeed, CYP3A4 has extremely broad substrate specificity and is responsible for the metabolism of ~50% of drugs in current use [16]. CYP3A4 is abundant (40–60%) in human liver, but absent in mouse or rat [17, 18]. This fact explains the far more rapid hydroxylation of PTI in HLMs than in rodent microsomes.

On the other hand, *O*-demethylation of PTI is primarily catalyzed by CYP2D6. CYP2D6 substrate binding is uniquely governed by an ion-pair interaction between a positively charged nitrogen atom and a negatively charged Asp^{301} residue [19]. Thus, the nitrogen atom in the IND moiety of PTI may play an important role in its interaction with CYP2D6 and the subsequent *O*-desmethylation of PTI. In contrast to its hydroxylation reaction, PTI is more rapidly O-demethylated in rat liver microsomes than in HLMs. This observation reflects the low abundance (2%) of CYP2D6 in human liver [20]. Our observation that the hydroxylation and *O*-demethylation of PTI are catalyzed by distinct CYP isoforms not only suggests that different molecular mechanisms are involved in these two reactions, but also demonstrates the unique CYP-catalyzed reaction specificity within a given substrate.

In contrast to PTI, IND (parent compound of PTI) is primarily *O*-demethylated by CYP2C9, which prefers acidic substrates like IND [21]. The interaction of Arg^{108} of CYP2C9 with the acidic ligands is critical for its substrate binding [22]. CYP2C9 is abundant in the human but absent in mouse or rat [18], which explains our observation that the IND was *O*-demethylated far more rapidly in HLMs than in rodent microsomes (Fig. 1B). The differential metabolism of PTI and IND by distinct CYP isoforms is primarily due to their strikingly different physicochemical properties, such as acidity and lipophilicity. As is the case with PTI and IND, CYP3A4 primarily catalyzed the hydroxylation of phospho-ibuprofen, whereas CYP2C9 exclusively hydroxylated ibuprofen [23]. These observations account, at least in part, for the characteristic metabolic profiles and pharmacokinetic properties of phospho-NSAIDs [23].

CES- and CYP-catalyzed hydrolysis and *O*-demethylation of PTI introduce polar –COOH and – OH functional groups, which are recognized by phase II conjugation enzymes for acyl glucuronidation and sulfation reactions, respectively. We detected two acyl glucuronides (IND glucuronide and demethyl-IND glucuronide) and demethyl-IND sulfate in the plasma of IND-and PTI-treated rats. To our knowledge, this is the first report of the sulfated metabolite derived from IND. These phase II conjugation reactions substantially enhance drug hydrophilicity, which generally facilitates drug elimination and detoxification. However, both glucuronidation [24] and sulfation reactions [25] have also been implicated in substrate activation and reactivity.

N-debenzoylation is a minor metabolic reaction for PTI and IND, involving the hydrolysis of an amide bond to form debenzoyl-PTI and debenzoyl-IND, respectively. This reaction is presumably catalyzed by an amidase/esterase, and is therefore NADPH-independent. In contrast, CYP-catalyzed *O*-demethylation of PTI and IND is NADPH-dependent. Similar to our observations, CYP-catalyzed *O*-deethylation of a phosphoric acid ester compound is NADPH-dependent, while esterase-catalyzed hydrolysis of its amide bond is NADPH-independent [26].

The metabolic fate of PTI has important implications for its efficacy. CYP3A4-mediated hydroxylation of PTI at its tyrosol moiety may contribute to its potent biological activity. Unlike tyrosol, hydroxy-tyrosol is a polyphenol that possess anti-inflammatory and anti-cancer activities [27]. Hydroxy-tyrosol has been shown to induce cancer cell apoptosis, inhibit cell proliferation and prevent cancer metastasis. Its molecular targets include ERK1/2, cyclin D1, 5- and 12-lipooxygenase [28, 29]. Given the significant biological activities of hydroxy-tyrosol, hydroxy-PTI may play an important role in cancer control.

On the other hand, CES-catalyzed hydrolysis of PTI may be detrimental to its bioactivity *in vivo*. We previously demonstrated that the intact PTI is more efficacious against cancer than conventional IND [13]. Given the strong CES activity in the intestine and liver, it is not surprising that intact PTI cannot be found following its oral administration in rats. It is thus conceivable that the bioactivity of PTI can be further improved if co-administered with CES inhibitors or formulated in nanocarriers that protect PTI from hydrolysis [30].

In summary, PTI undergoes extensive metabolic transformations *in vitro* and *in vivo*, generating numerous metabolites. Our results reveal significant differences in its metabolism between humans and laboratory rodents, which would help to predict clinical outcomes based on preclinical animal data.

Acknowledgments

This work was supported by the National Institute of Health Grant R01CA139454. We thank R. Rieger and T. Koller, Stony Brook University, for their expert LC-MS/MS analysis and the shared instrumentation grant, NIH/NCRR 1 S10 RR023680-1. We also thank Carol Ann Amella for critically reading the manuscript.

Abbreviations

CES	carboxylesterase
CYP	cytochrome P450
DFP	diisopropyl fluorophosphates
HLMs	human liver microsomes
IND	indomethacin
PTI	phospho-tyrosol-indomethacin
UGT	UDP-glucuronosyltransferases

References

1. Grivennikov SI, Greten FR, Karin M. Immunity, inflammation, and cancer. Cell. 2010; 140:883–899. [PubMed: 20303878]
2. Hial V, Horakova Z, Shaff FE, Beaven MA. Alteration of tumor growth by aspirin and indomethacin: studies with two transplantable tumors in mouse. European journal of pharmacology. 1976; 37:367–376. [PubMed: 954814]
3. Narisawa T, Sato M, Tani M, Kudo T, Takahashi T, Goto A. Inhibition of development of methylnitrosourea-induced rat colon tumors by indomethacin treatment. Cancer research. 1981; 41:1954–1957. [PubMed: 7214363]
4. Connolly JM, Liu XH, Rose DP. Dietary linoleic acid-stimulated human breast cancer cell growth and metastasis in nude mice and their suppression by indomethacin, a cyclooxygenase inhibitor. Nutrition and cancer. 1996; 25:231–240. [PubMed: 8771566]

5. Hida T, Leyton J, Makheja AN, Ben-Av P, Hla T, Martinez A, et al. Non-small cell lung cancer cycloxygenase activity and proliferation are inhibited by non-steroidal antiinflammatory drugs. Anticancer research. 1998; 18:775–782. [PubMed: 9615719]
6. Fischer SM, Lo HH, Gordon GB, Seibert K, Kelloff G, Lubet RA, et al. Chemopreventive activity of celecoxib, a specific cyclooxygenase-2 inhibitor, and indomethacin against ultraviolet light-induced skin carcinogenesis. Molecular carcinogenesis. 1999; 25:231–240. [PubMed: 10449029]
7. Narisawa T, Satoh M, Sano M, Takahashi T. Inhibition of initiation and promotion by N-methylnitrosourea-induced colon carcinogenesis in rats by non-steroid anti-inflammatory agent indomethacin. Carcinogenesis. 1983; 4:1225–1227. [PubMed: 6616752]
8. Ackerstaff E, Gimi B, Artemov D, Bhujwalla ZM. Anti-inflammatory agent indomethacin reduces invasion and alters metabolism in a human breast cancer cell line. Neoplasia. 2007; 9:222–235. [PubMed: 17401462]
9. Kato T, Fujino H, Oyama S, Kawashima T, Murayama T. Indomethacin induces cellular morphological change and migration via epithelial-mesenchymal transition in A549 human lung cancer cells: A novel cyclooxygenase-inhibition-independent effect. Biochemical pharmacology. 2011
10. Shiff SJ, Koutsos MI, Qiao L, Rigas B. Nonsteroidal antiinflammatory drugs inhibit the proliferation of colon adenocarcinoma cells: effects on cell cycle and apoptosis. Experimental cell research. 1996; 222:179–188. [PubMed: 8549662]
11. Zhou D, Papayannis I, Mackenzie GG, Alston N, Ouyang N, Huang L, et al. The anticancer effect of phospho-tyrosol-indomethacin (MPI 621), a novel phospho-derivative of indomethacin: In vitro and in vivo studies. Carcinogenesis. 2013
12. Sweeney BP, Bromilow J. Liver enzyme induction and inhibition: implications for anaesthesia. Anaesthesia. 2006; 61:159–177. [PubMed: 16430569]
13. Wong CC, Cheng KW, Xie G, Zhou D, Zhu CH, Constantinides PP, et al. Carboxylesterases 1 and 2 hydrolyze phospho-nonsteroidal anti-inflammatory drugs: relevance to their pharmacological activity. The Journal of pharmacology and experimental therapeutics. 2012; 340:422–432. [PubMed: 22085648]
14. Hosokawa M. Structure and catalytic properties of carboxylesterase isozymes involved in metabolic activation of prodrugs. Molecules. 2008; 13:412–431. [PubMed: 18305428]
15. Nishimura M, Naito S. Tissue-specific mRNA expression profiles of human phase I metabolizing enzymes except for cytochrome P450 and phase II metabolizing enzymes. Drug metabolism and pharmacokinetics. 2006; 21:357–374. [PubMed: 17072089]
16. Kapelyukh Y, Paine MJ, Marechal JD, Sutcliffe MJ, Wolf CR, Roberts GC. Multiple substrate binding by cytochrome P450 3A4: estimation of the number of bound substrate molecules. Drug metabolism and disposition: the biological fate of chemicals. 2008; 36:2136–2144. [PubMed: 18645035]
17. Davis MP, Homsi J. The importance of cytochrome P450 monooxygenase CYP2D6 in palliative medicine. Supportive care in cancer : official journal of the Multinational Association of Supportive Care in Cancer. 2001; 9:442–451. [PubMed: 11585271]
18. Martignoni M, Groothuis GM, de Kanter R. Species differences between mouse, rat, dog, monkey and human CYP-mediated drug metabolism, inhibition and induction. Expert opinion on drug metabolism & toxicology. 2006; 2:875–894. [PubMed: 17125407]
19. Ellis SW, Hayhurst GP, Smith G, Lightfoot T, Wong MM, Simula AP, et al. Evidence that aspartic acid 301 is a critical substrate-contact residue in the active site of cytochrome P450 2D6. The Journal of biological chemistry. 1995; 270:29055–29058. [PubMed: 7493924]
20. Pelkonen O, Maenpaa J, Taavitsainen P, Rautio A, Raunio H. Inhibition and induction of human cytochrome P450 (CYP) enzymes. Xenobiotica; the fate of foreign compounds in biological systems. 1998; 28:1203–1253.
21. Nakajima M, Inoue T, Shimada N, Tokudome S, Yamamoto T, Kuroiwa Y. Cytochrome P450 2C9 catalyzes indomethacin O-demethylation in human liver microsomes. Drug metabolism and disposition: the biological fate of chemicals. 1998; 26:261–266. [PubMed: 9492390]

22. Dickmann LJ, Locuson CW, Jones JP, Rettie AE. Differential roles of Arg97, Asp293, and Arg108 in enzyme stability and substrate specificity of CYP2C9. Molecular pharmacology. 2004; 65:842–850. [PubMed: 15044613]

23. Xie G, Wong CC, Cheng KW, Huang L, Constantinides PP, Rigas B. Regioselective oxidation of phospho-NSAIDs by human cytochrome P450 and flavin monooxygenase isoforms: implications for their pharmacokinetic properties and safety. British journal of pharmacology. 2012; 167:222–232. [PubMed: 22489789]

24. Johnson CH, Wilson ID, Harding JR, Stachulski AV, Iddon L, Nicholson JK, et al. NMR spectroscopic studies on the in vitro acyl glucuronide migration kinetics of Ibuprofen ((+/−)-(R,S)-2-(4-isobutylphenyl) propanoic acid), its metabolites, and analogues. Analytical chemistry. 2007; 79:8720–8727. [PubMed: 17944439]

25. Falany CN. Sulfation and sulfotransferases. Introduction: changing view of sulfation and the cytosolic sulfotransferases. The FASEB journal : official publication of the Federation of American Societies for Experimental Biology. 1997; 11:1–2.

26. Morioka Y, Otsu M, Naito S, Imai T. Phosphonate O-deethylation of [4-(4-bromo-2-cyano-phenylcarbamoyl) benzyl]-phosphonic acid diethyl ester, a lipoprotein lipase-promoting agent, catalyzed by cytochrome P450 2C8 and 3A4 in human liver microsomes. Drug metabolism and disposition: the biological fate of chemicals. 2002; 30:301–306. [PubMed: 11854149]

27. Hashim YZ, Eng M, Gill CI, McGlynn H, Rowland IR. Components of olive oil and chemoprevention of colorectal cancer. Nutrition reviews. 2005; 63:374–386. [PubMed: 16370222]

28. Corona G, Deiana M, Incani A, Vauzour D, Dessi MA, Spencer JP. Hydroxytyrosol inhibits the proliferation of human colon adenocarcinoma cells through inhibition of ERK1/2 and cyclin D1. Molecular nutrition & food research. 2009; 53:897–903. [PubMed: 19685549]

29. de la Puerta R, Ruiz Gutierrez V, Hoult JR. Inhibition of leukocyte 5-lipoxygenase by phenolics from virgin olive oil. Biochemical pharmacology. 1999; 57:445–449. [PubMed: 9933033]

30. Nie T, Wong CC, Alston N, Aro P, Constantinides PP, Rigas B. Phospho-ibuprofen (MDC-917) incorporated in nanocarriers: anti-cancer activity in vitro and in vivo. British journal of pharmacology. 2012; 166:991–1001. [PubMed: 22141583]

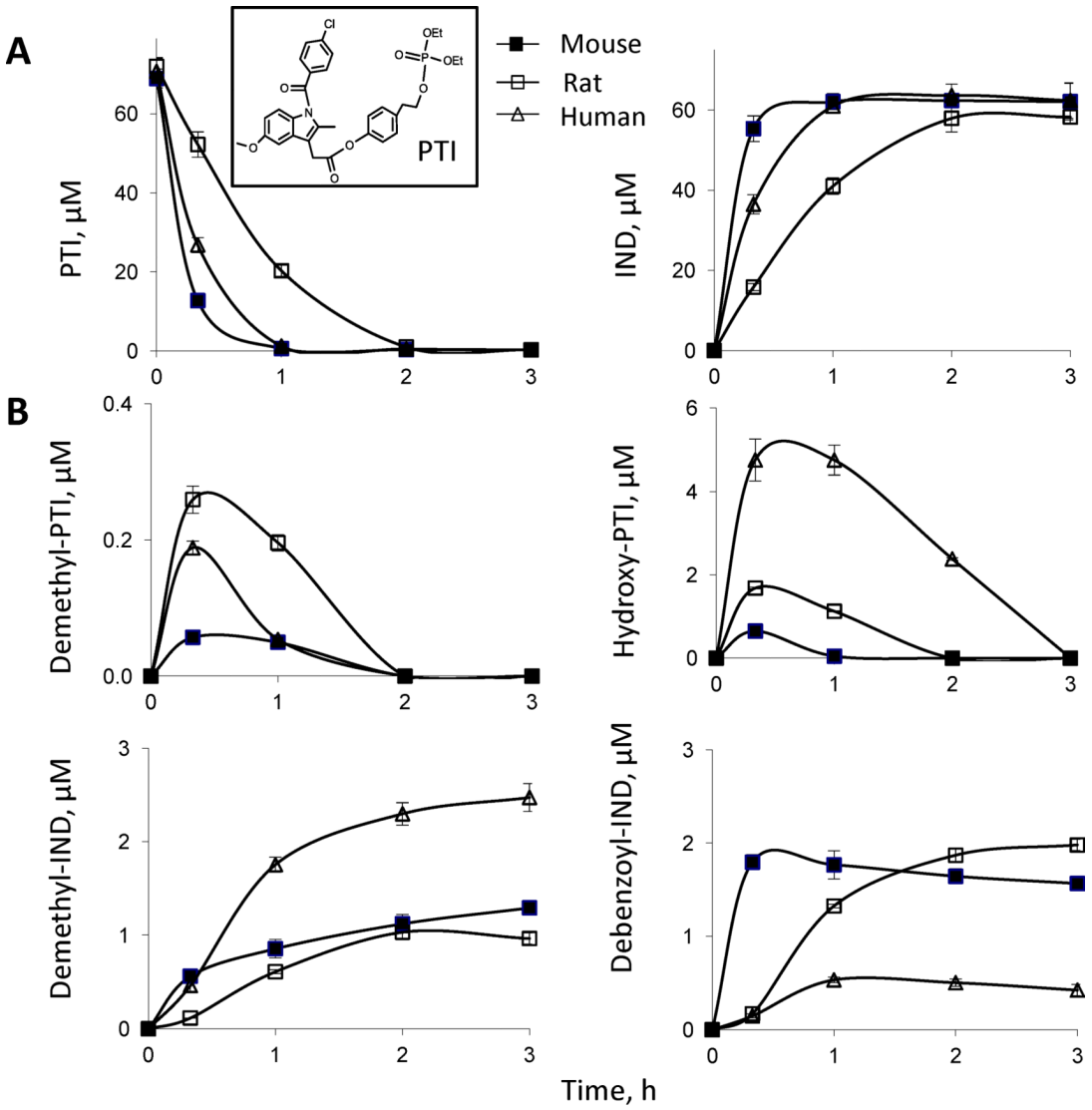

C Metabolite levels of PTI in HLM 20 min after reaction initiation

	Hydroxy-PTI	Demethyl-PTI	Demethyl-IND	Debenzoyl-IND
	Microsomal level, n M			
NADPH (+)	4,760	189	461	149
NADPH (-)	Not detectable			140

Fig. 1. Kinetics of PTI metabolism by mouse, rat and human liver microsomes

A: Time courses of the levels of PTI and IND in PTI-treated liver microsomes. PTI (75 μM) was incubated with mouse, rat and human liver microsomes (protein concentration 0.5 mg/ml) at 37°C for up to 3 h. PTI and its metabolites were extracted at the designated time points and assayed using HPLC. **Inset**, the structure of PTI. **B:** Time course of metabolite formation in PTI-treated liver microsomes. **C:** Comparison of metabolite formation in PTI-treated HLMs in the presence (+) versus absence (−) of NADPH, 20 min after the initiation of the reaction.

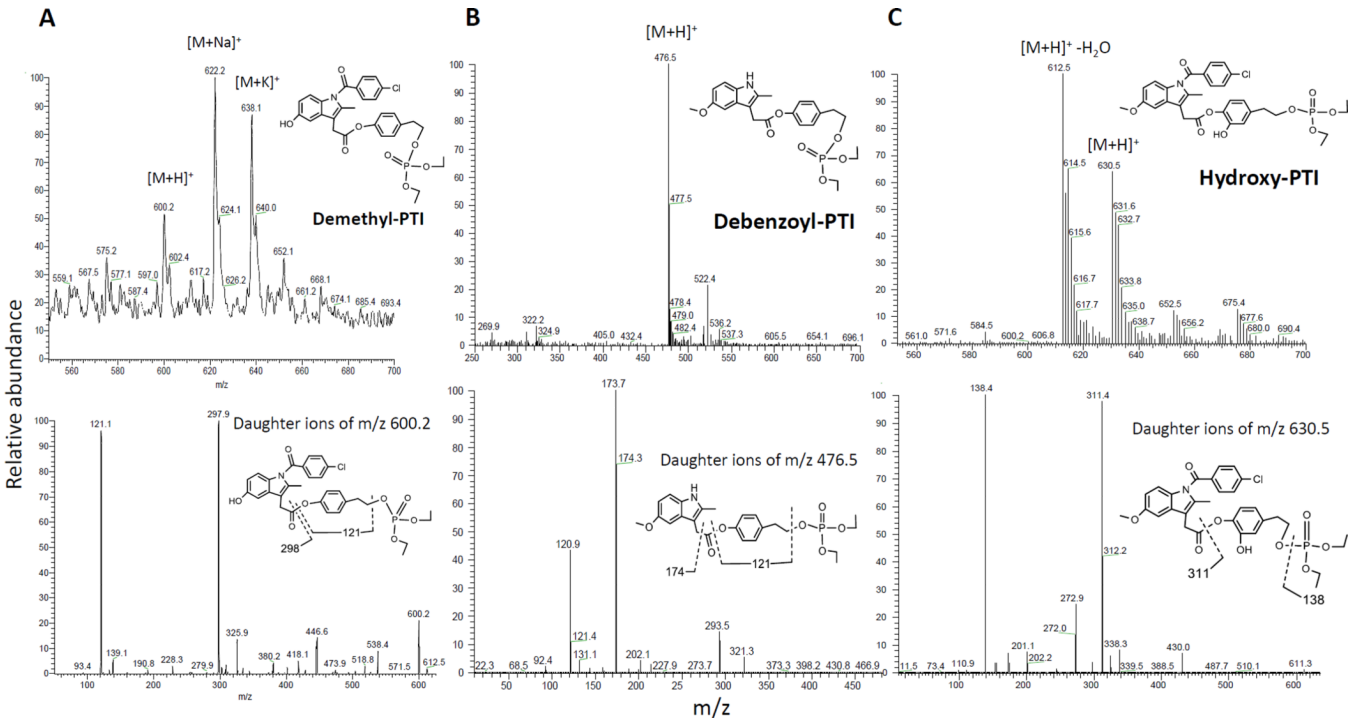

Fig. 2. Identification of the microsomal metabolites of PTI using LC-MS/MS analysis

MS (*top*) and MS_2 (*bottom*) ion spectra were shown. **A:** *Top*, the protonated demethyl-PTI was observed at *m/z* 600.2. *Bottom*, the ion above was fragmented to generate ions at *m/z* 121.1 and 297.9. **B:** *Top*, the protonated debenzoyl-PTI was observed at *m/z* 476.5. *Bottom*, the ion above was fragmented to generate ions at *m/z* 120.9 and 173.7 **C:** *Top*, the protonated hydroxy-PTI was observed at *m/z* 630.5. *Bottom*, the ion above was fragmented to generate ions at *m/z* 138.4 and 311.4.

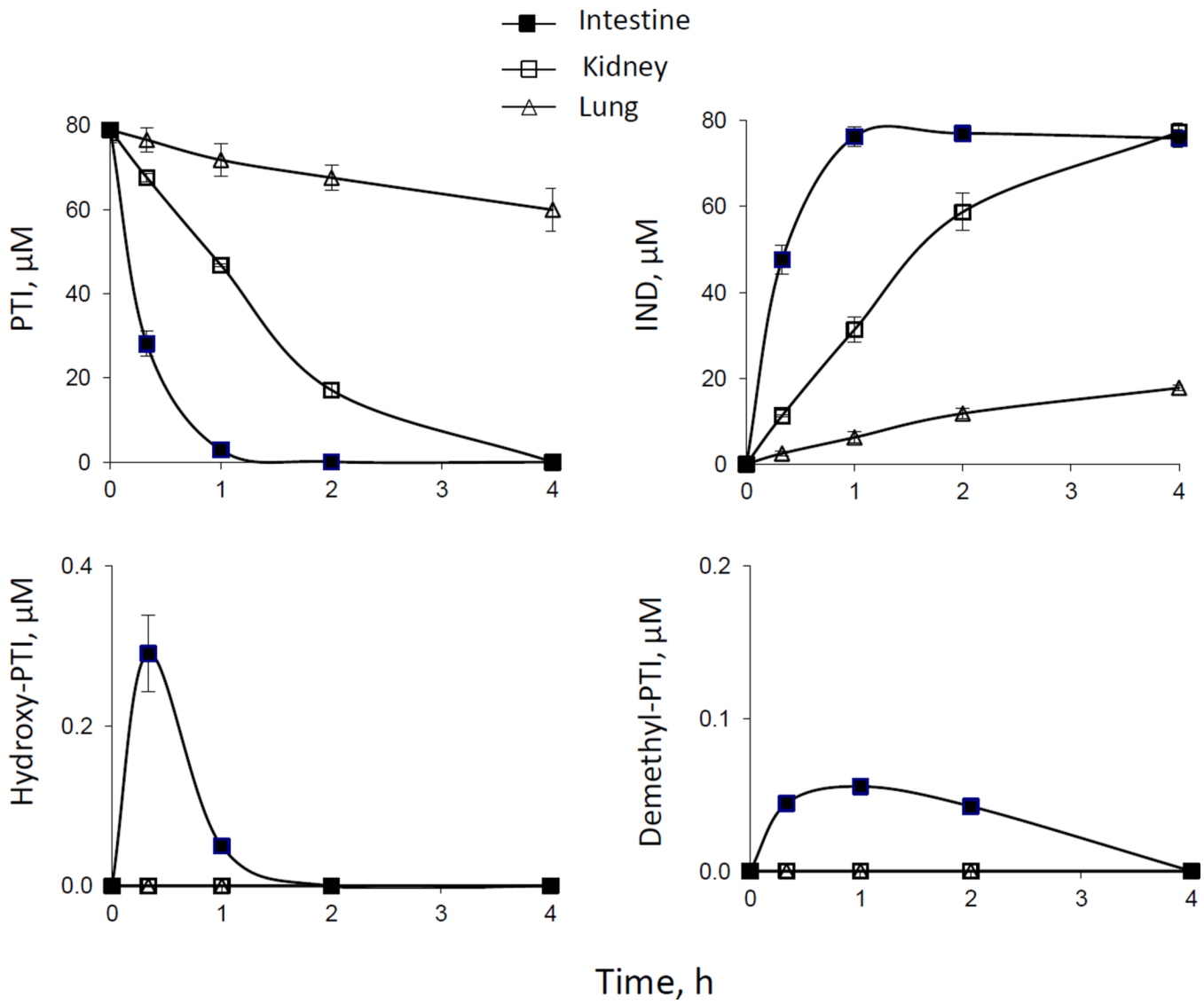

Fig. 3. Kinetics of PTI metabolism by human intestine, kidney, and lung microsomes

Time courses of the levels of PTI and its metabolites in PTI-treated human microsomes. PTI (80 μM) was incubated with human intestine, kidney and lung microsomes (protein concentration 0.25 mg/ml) at 37°C for up to 4 h. PTI and its metabolites were extracted at the designated time points and assayed as described in Methods.

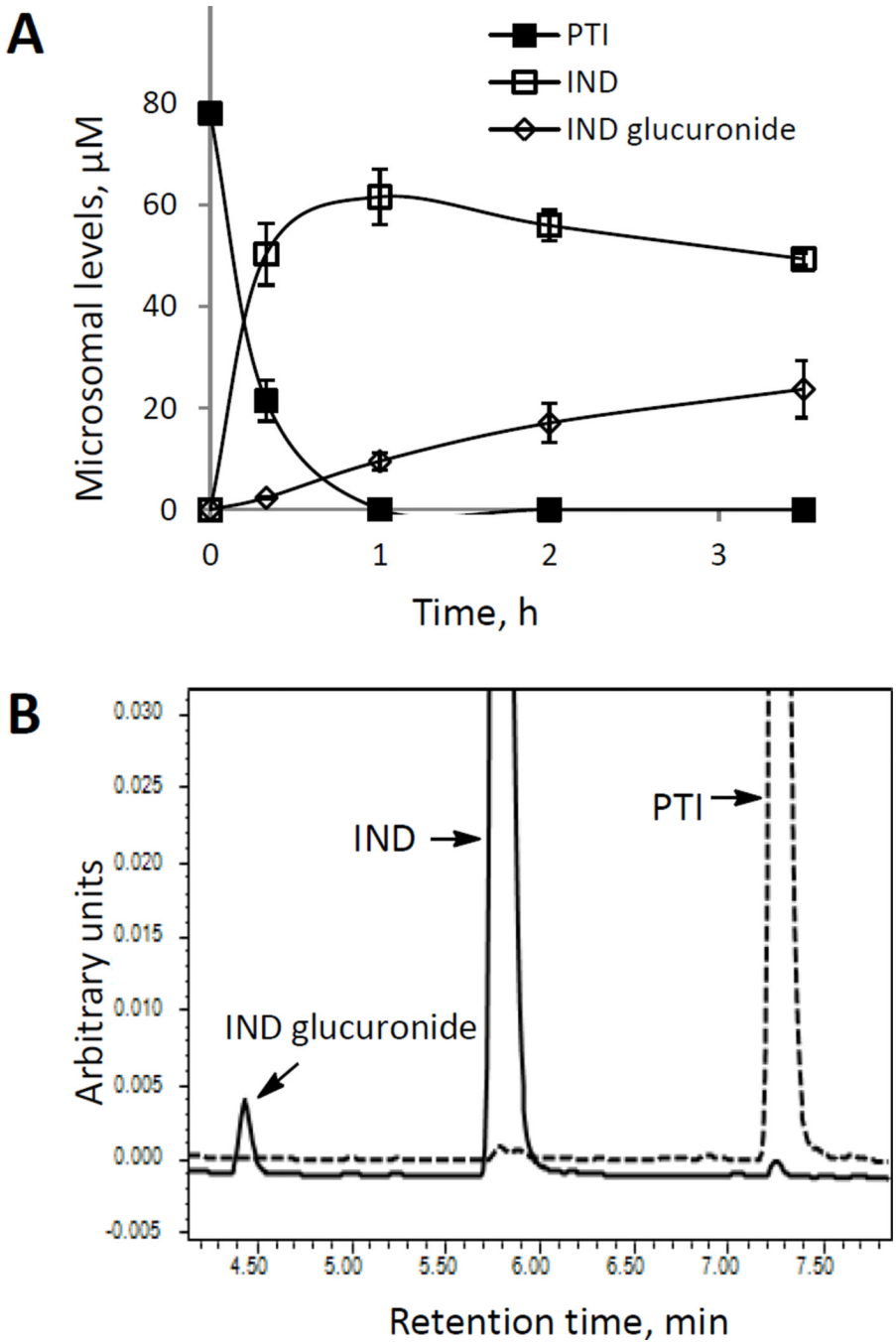

Fig. 4. Glucuronidation of PTI by human liver microsomes

A: Time course of the levels of PTI and its metabolites in PTI-treated HLMs in the presence of UDP-glucuronic acid. **B**: Comparison of glucuronide formation from PTI versus IND in HLMs treated with the esterase inhibitor DFP. HLMs were treated with PTI (dotted line) or IND (solid line) in the presence of DFP for 2 h, and the metabolite levels were determined by HPLC. The respective chromatograms are shown. The off-scale peak values of IND and PTI were 0.41 and 0.25 units, respectively.

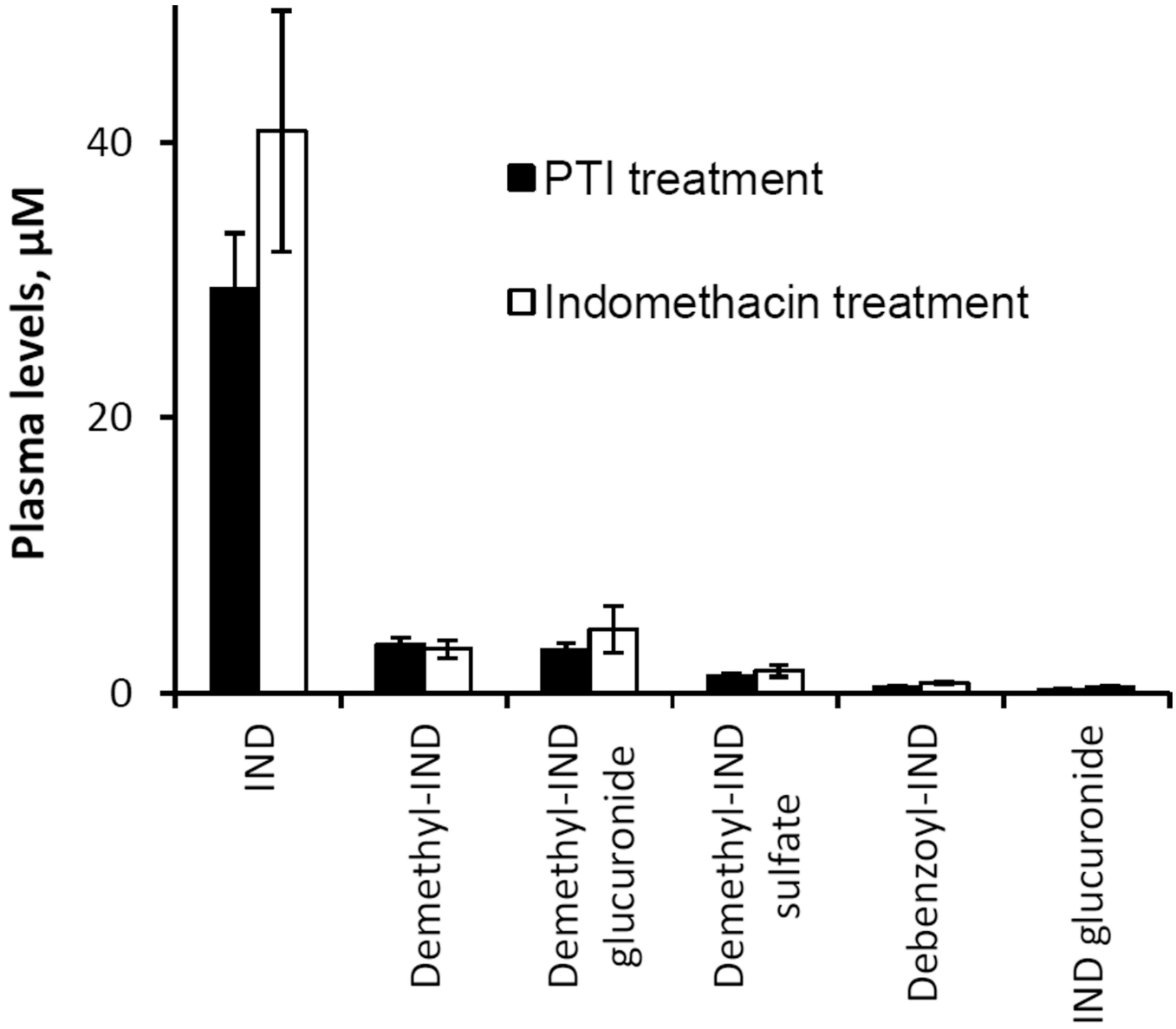

Fig. 5. Drug levels in the plasma of PTI- or IND-treated rats

Equimolar amounts of PTI (10 mg/kg) or IND (5 mg/kg) in corn oil were administered orally to rats, and their blood was obtained 3 h later. Plasma levels of the metabolites were determined using HPLC, as described in Methods.

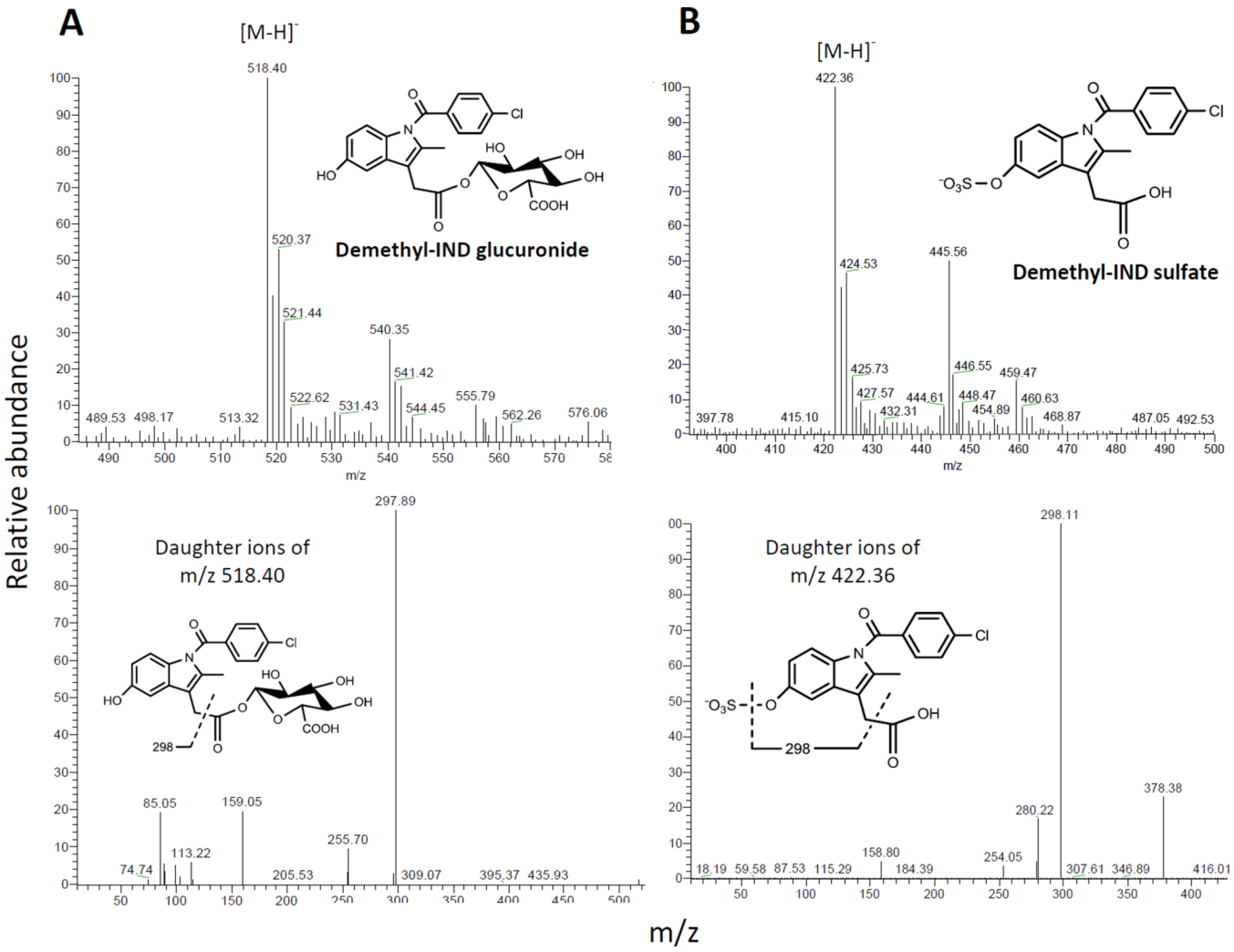

Fig. 6. Identification of the conjugated metabolites derived from demethyl-IND

MS (*top*) and MS_2 (*bottom*) ion spectra were shown. **A:** *Top*, the deprotonated demethyl-IND glucuronide was observed at *m/z* 518.40. *Bottom*, the ion above was fragmented at its glucuronide bond to generate an ion at *m/z* 297.89. **B:** *top*, the deprotonated demethyl-IND sulfate was observed at *m/z* 422.36. *Bottom*, the ion above was fragmented at its sulfate bond to generate an ion at *m/z* 298.11 (Fig. 6B).

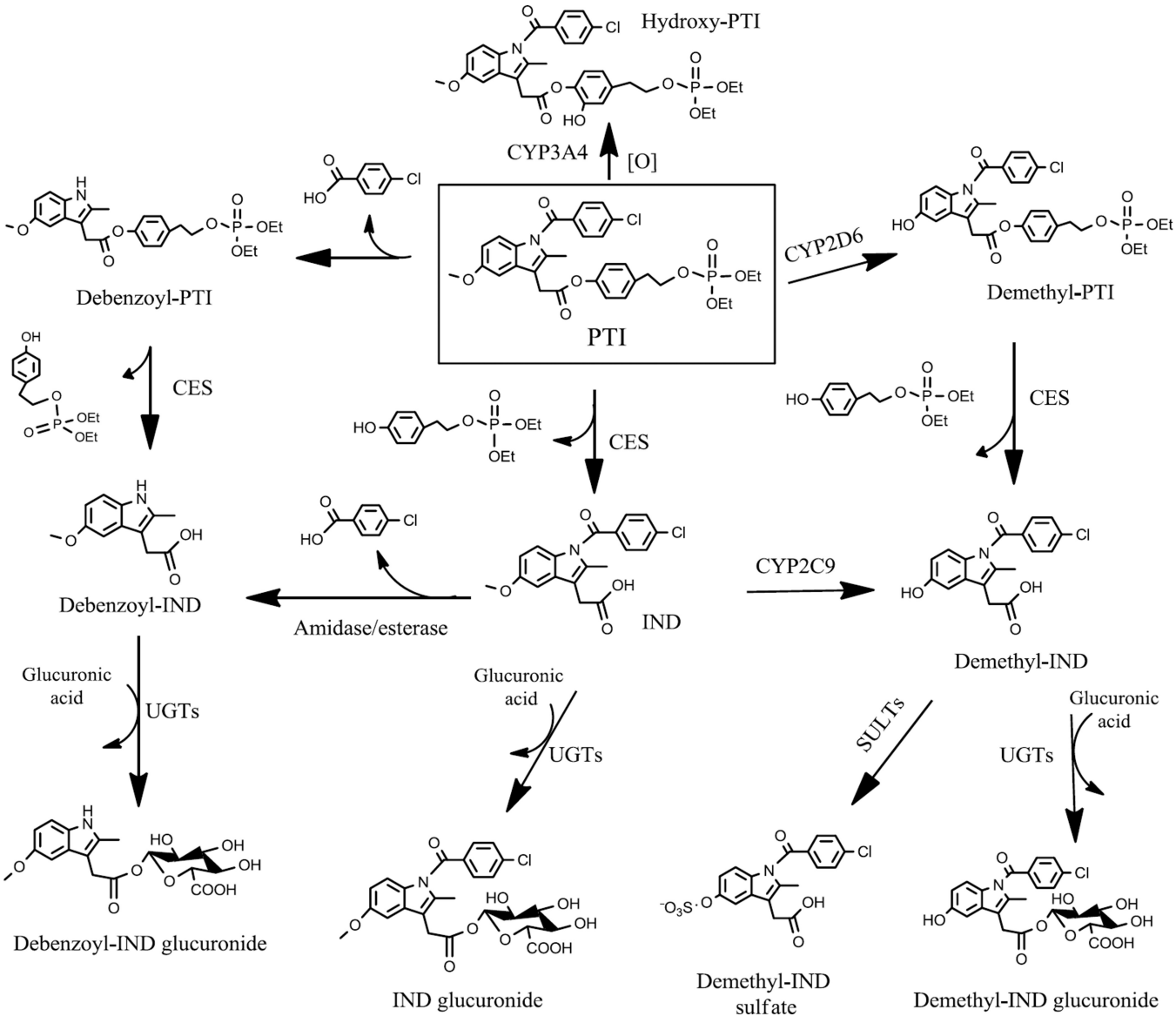

Fig. 7. Overall metabolic pathways of PTI *in vitro* and *in vivo*

PTI undergoes hydrolysis, hydroxylation, *O*-demethylation and *N*-debenzoylation reactions to generate IND, hydroxy-PTI, demethyl-PTI and debenzoyl-PTI, respectively. The resulting IND can be transformed to demethyl-IND and debenzoyl-IND, which, in turn, can be glucuronidated. Demethyl-IND can also be sulfated. *SULTs, sulfotransferases*.

Table 1

The stability ($t_{1/2}$ and CL_{int}) of PTI in mouse, rat and human microsomes from various tissues.

	$t_{1/2}$ *min*	CL_{int} *ml/min/g*
Mouse liver microsomes	8.0	172.4
Rat liver microsomes	37.6	36.9
Human liver microsomes	13.9	100.0
Human intestine microsomes	13.2	210.0
Human kidney microsomes	77.3	35.9
Human lung microsomes	348.0	8.0

Table 2

Kinetic parameters for the hydroxylation and *O*-demethylation reactions of PTI by human recombinant CYPs.

	Hydroxylation of PTI			O-demethylation of PTI		
	K_m	V_{max}	V_{max}/K_m	K_m	V_{max}	V_{max}/K_m
	μM	*pmol/min/ pmol CYP*	*μl/min/pmol CYP*	*μM*	*pmol/min/ pmol CYP*	*μl/min/pmol CYP*
CYP1A2	ND			ND		
CYP2C9	ND			ND		
CYP2C19	ND			ND		
CYP2D6	ND			4.0	70.0	17.5
CYP3A4	2.5	27.5	27.5	44.5	1.5	0.03

ND, Not detectable